Catch bonds govern adhesion through L-selectin at threshold shear

Tadayuki Yago,[1] Jianhua Wu,[3] C. Diana Wey,[4] Arkadiusz G. Klopocki,[1] Cheng Zhu,[4,5] and Rodger P. McEver[1,2]

[1]Cardiovascular Biology Research Program, Oklahoma Medical Research Foundation, and [2]Department of Biochemistry and Molecular Biology, Oklahoma Center for Medical Glycobiology, University of Oklahoma Health Sciences Center, Oklahoma City, OK 73104
[3]School of Life Sciences, Zhongshan University, Guangzhou 510275, China
[4]Coulter Department of Biomedical Engineering and [5]Woodruff School of Mechanical Engineering, Georgia Institute of Technology, Atlanta, GA 30332

Flow-enhanced cell adhesion is an unexplained phenomenon that might result from a transport-dependent increase in on-rates or a force-dependent decrease in off-rates of adhesive bonds. L-selectin requires a threshold shear to support leukocyte rolling on P-selectin glycoprotein ligand-1 (PSGL-1) and other vascular ligands. Low forces decrease L-selectin–PSGL-1 off-rates (catch bonds), whereas higher forces increase off-rates (slip bonds). We determined that a force-dependent decrease in off-rates dictated flow-enhanced rolling of L-selectin–bearing microspheres or neutrophils on PSGL-1. Catch bonds enabled increasing force to convert short-lived tethers into longer-lived tethers, which decreased rolling velocities and increased the regularity of rolling steps as shear rose from the threshold to an optimal value. As shear increased above the optimum, transitions to slip bonds shortened tether lifetimes, which increased rolling velocities and decreased rolling regularity. Thus, force-dependent alterations of bond lifetimes govern L-selectin–dependent cell adhesion below and above the shear optimum. These findings establish the first biological function for catch bonds as a mechanism for flow-enhanced cell adhesion.

Introduction

Cell adhesion occurs under kinetic and mechanical constraints, which are particularly evident during lymphocyte homing or leukocyte trafficking into sites of inflammation (Vestweber and Blanks, 1999; McEver, 2001, 2002). Flowing leukocytes tether to and roll on vascular surfaces, a process that requires rapid formation and dissociation of adhesive bonds. Due to the hydrodynamic environment, these bonds are subjected to forces that affect their off-rates. Interactions of selectins with cell surface glycoconjugates mediate leukocyte rolling. L-selectin, expressed on leukocytes, binds to ligands on endothelial cells and on other leukocytes. P-selectin and E-selectin, expressed on activated platelets and/or endothelial cells, recognize ligands on leukocytes or platelets. The major leukocyte ligand for P-selectin and L-selectin is P-selectin glycoprotein ligand-1 (PSGL-1; McEver, 2001, 2002).

Selectins require a threshold shear to support cell adhesion (Finger et al., 1996; Alon et al., 1997; Lawrence et al., 1997). As shear drops below the threshold level, fewer flowing cells tether, and the cells roll more rapidly and begin to detach. The shear threshold requirement for L-selectin to support rolling is particularly striking and may prevent inappropriate leukocyte aggregation during vascular stasis. Other cell adhesion systems also exhibit flow enhancement. For example, platelets require arterial flow rates to adhere to von Willebrand factor on damaged vascular surfaces (Savage et al., 1996; Doggett et al., 2002). In addition, many enteric bacteria require a minimum flow rate to adhere to intestinal epithelia, which likely prevents pathological attachments to bladder mucosa during stasis (Thomas et al., 2002). Therefore, flow-enhanced adhesion is a biologically important process that may be used by many cells.

Address correspondence to Cheng Zhu, Woodruff School of Mechanical Engineering, Georgia Institute of Technology, Atlanta, GA 30332-0405. Tel.: (404) 894-3269. Fax: (404) 385-1397. email: cheng.zhu@me.gatech.edu; or Rodger P. McEver, Cardiovascular Biology Research Program, Oklahoma Medical Research Foundation, 825 N.E. 13th Street, Oklahoma City, OK 73104. Tel.: (405) 271-6480. Fax: (405) 271-3137. email: rodger-mcever@omrf.ouhsc.edu

Key words: leukocyte; PSGL-1; inflammation; lymphocyte homing; selectin

The shear threshold requirement seems counterintuitive because increasing shear elevates the dislodging force applied to adhesive bonds. Nevertheless, cells roll more slowly and more regularly until an optimal shear is reached where rolling velocity is minimal. This paradoxical phenomenon has not been satisfactorily explained despite the widespread interest that it has generated. The prevailing hypothesis is that bond formation is enhanced by a flow-dependent increase in the on-rates of adhesive bonds. This might occur by shear rate–dependent transport of adhesion molecules to their ligands so that new bonds form before previous bonds dissociate (Finger et al., 1996; Chang and Hammer, 1999; Chen and Springer, 1999), or by shear stress–dependent enlargement of the cell surface contact area that brings more adhesion molecules into proximity so they can form new bonds (Lawrence et al., 1997; Evans et al., 2001; Zhao et al., 2001). An alternative hypothesis is that force slows bond off-rates, which lengthens bond lifetimes and thus stabilizes rolling. Most workers dismissed the latter possibility because "catch bonds," whose lifetimes are prolonged by force (Dembo et al., 1988), had not been experimentally demonstrated. By contrast, "slip bonds" (Dembo et al., 1988), whose lifetimes are shortened by force (Bell, 1978), have been observed frequently, particularly in interactions involving selectins (Alon et al., 1995, 1997; Evans et al., 2001; Ramachandran et al., 2001; Doggett et al., 2002). One paper showed that shear stress increases bacterial adhesion to target cells, but did not establish whether alterations in on-rates or off-rates of adhesive bonds cause this effect (Thomas et al., 2002). Nevertheless, it was speculated that catch bonds confer flow-enhanced bacterial adhesion, whereas shear rate–mediated transport enables flow-enhanced leukocyte adhesion (Isberg and Barnes, 2002). However, subsequent analyses demonstrated that P-selectin and L-selectin form catch bonds with PSGL-1 at forces that begin at the respective threshold shear that supports leukocyte rolling and end at the respective optimal force where bond lifetimes reach maximum (Marshall et al., 2003; Sarangapani et al., 2004). At forces above the optimal values, P-selectin and L-selectin dissociate from PSGL-1 with characteristics of slip bonds. Transitions from catch bonds to slip bonds might explain why rises in shear first increase rolling regularity while slowing rolling velocities, and then decrease rolling regularity while increasing rolling velocities. The catch–slip bond transition occurs at a higher force range for L-selectin than for P-selectin, consistent with the higher shear threshold for L-selectin–dependent rolling (Marshall et al., 2003; Sarangapani et al., 2004). The experimental demonstration of catch bonds suggested (but did not prove) that they contribute to flow-enhanced adhesion. Indeed, a recent report dismisses the catch bond mechanism and proposes that L-selectin tethers that form at the shear threshold are stabilized by a transport-mediated increase in bond number (Dwir et al., 2003).

Here, we measured the independent effects of transport, tether force, and contact area on transient tether off-rates and on rolling of L-selectin–bearing microspheres or cells on PSGL-1 below and above the shear optimum. Our results demonstrate that catch bonds govern rolling below the optimal shear, whereas slip bonds govern rolling above the optimal shear. These data identify catch bonds as a fundamental mechanism underlying the shear threshold phenomenon.

Results

Governing parameters of adhesion under flow

We studied rolling of neutrophils or microspheres bearing L-selectin on immobilized soluble PSGL-1 (sPSGL-1) at flow rates below and above the optimal value. To examine the mechanisms for the shear threshold requirement, we exploited the biophysical parameters that govern adhesion under flow (Fig. 1). Shear stress, the product of shear rate and viscosity, applies a resultant force F_s and a torque T_s to the adherent sphere (or cell), both of which increase as the rolling sphere slows and reach maximum when the sphere stops. F_s and T_s are balanced by tensile forces on the adhesive bonds at the trailing edge of a tethered sphere (F_t), which alter the off-rates of the bonds, and by compressive forces at the sphere bottom (F_c), which enlarge the contact area of a deformable cell, but not of a fixed, nondeformable cell or a rigid microsphere (Fig. 1 A). At the same shear rate, increasing the viscosity increases the shear stress, and in turn the tether force on a sphere of constant size. At the same shear stress, more force is applied to the adhesive tether of a large sphere than a small sphere. At low L-selectin or sPSGL-1 densities, a sphere can form a transient adhesive tether but then returns to the fluid stream after the tether dissociates. At higher densities, the sphere rolls as new bonds replace those that dissociate at the trailing edge. A rolling sphere stops when the adhesive bond (or bond cluster) can withstand the force required to balance the maximal F_s and T_s (Fig. 1 B). After dissociation of this bond (or the last bond in a bond cluster), the sphere accelerates as it pivots on a newly formed bond upstream and then decelerates as force develops in the bond. The sphere stops again if the new bond lives long enough to generate sufficient force to counter the maximal F_s and T_s. If the bond dissociates prematurely, the sphere accelerates again before it can stop.

We correlated transient tether lifetimes, which allow determination of off-rates of single adhesive bonds, with detailed rolling properties below and above the flow optimum. To examine the contributions of on-rate and off-rate to the shear threshold requirement, we independently altered wall shear rate, wall shear stress, tether force, and contact area at flow rates below and above the optimal value. Thus, we compared media with or without 6% Ficoll, which changes viscosity, and hence wall shear stress and tether force by 2.6-fold without changing wall shear rate; compared microspheres with radii of 3 or 1 μm, which changes tether force by ninefold without changing wall shear stress; and compared deformable neutrophils with rigid microspheres or fixed neutrophils, which changes contact area without changing tether force (Fig. 1 A).

Transitions between catch bonds and slip bonds govern mean rolling velocities below and above the optimal force

First, we studied mean rolling velocity, a global measure of rolling adhesion that changes as flow increases from the threshold to and above the optimal value. This parameter, measured at 30 frames per second (fps), was plotted against wall shear rate, wall shear stress, and tether force (Fig. 2). Essentially identical data were obtained when rolling was mea-
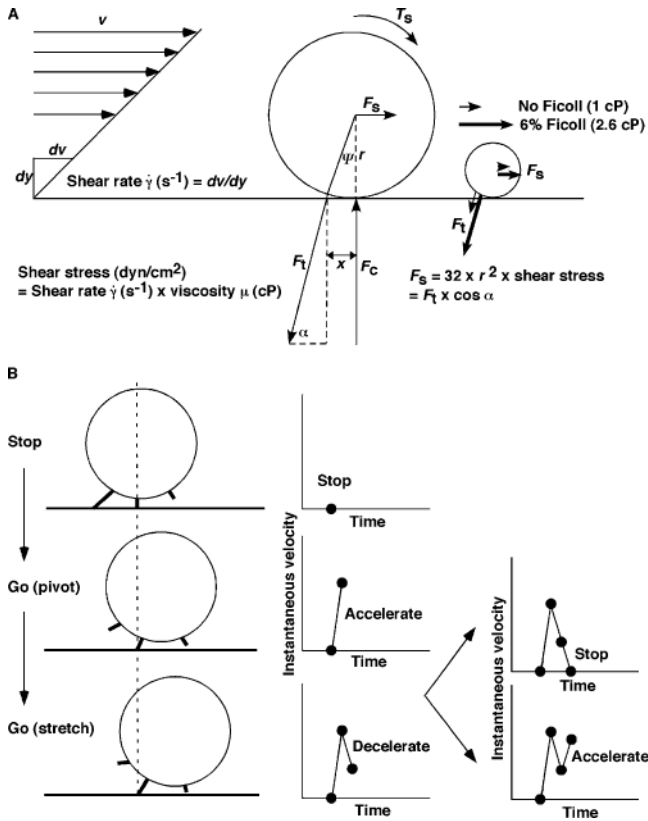
Figure 1.   **Parameters of rolling adhesion under flow.** (A) The rolling motions of a microsphere or neutrophil of radius r are governed by the balance of the resultant force (F_s) and torque (T_s) exerted by the flowing fluid, the tether force (F_t) applied through L-selectin–PSGL-1 bonds, and the contact force (F_c). The conversion of wall shear stress to F_t using the indicated variables is described in Materials and methods. Elevating the viscosity by addition of 6% Ficoll increases shear stress by 2.6-fold and therefore increases F_t on a sphere of constant size, as illustrated by the comparative lengths of the thin and thick vectors for F_t on the small sphere. At the same shear stress, F_t is ninefold greater for a sphere of 3-μm radius than for a sphere of 1-μm radius, as illustrated by the comparative lengths of the thin vectors for F_t on the large and small spheres. (B) A rolling sphere stops when the adhesive bond sustains the full load required to balance the maximum F_t and T_s. After the bond dissociates, the sphere accelerates as it pivots on a newly formed bond upstream and then decelerates as force develops in the bond. The sphere stops again if the new bond has sufficient strength to withstand the full load and lives long enough to survive loading, or it accelerates if the bond dissociates prematurely.

sured at 250 fps. The density of monomeric sPSGL-1 was 140 sites/μm^2 in the data shown here. A 2.3-fold increase in sPSGL-1 density on the flow chamber floor lowered rolling velocities, whereas a threefold decrease in L-selectin density on microspheres raised rolling velocities. However, alterations in molecular densities did not change the shapes of the plots or shift the relative positions of the minimum values of the plots (unpublished data). In the experiments shown, we altered viscosity by including 6% Ficoll of 400,000 M_r in the media. Inclusion of 9% Ficoll of 70,000 M_r increased viscosity by the same amount and produced identical changes in the velocity curves (unpublished data). The matching results with Ficoll of different sizes suggests that Ficoll acted solely through alterations in viscosity rather

than through unsuspected effects on L-selectin bonds. All plots exhibited similar biphasic curves in which the rolling velocity first decreased, reached a minimum, and then increased—a characteristic of the shear threshold phenomenon. The slopes of the ascending curves were steeper for microspheres and fixed neutrophils than for unfixed neutrophils. This suggests that fixation-sensitive cellular features, which may include increased contact area, stabilize rolling as shear is increased above the optimum (Yago et al., 2002). The minimal rolling velocity was slightly lower for microspheres (Fig. 2, A–C) than for neutrophils (Fig. 2, D–F), perhaps because of the lower L-selectin density on neutrophils (see Materials and methods). Plots of rolling velocity versus wall shear rate shifted for media of different viscosities, indicating that velocity did not scale with this transport parameter (Fig. 2, A and D). On the other hand, plots of rolling velocity versus wall shear stress matched closely for microspheres (Fig. 2 B) or neutrophils (Fig. 2 E) of the same radius despite the different viscosities used. Velocity versus wall shear stress plots shifted horizontally for microspheres of different radii (Fig. 2 B). This shift was due to differences in tether force applied to microspheres of different radii because all velocity curves aligned when plotted against tether force (Fig. 2, C and F). This scaling property demonstrates that tether force directly governs rolling velocity both below and above the optimal flow rate.

Tether force most likely governs rolling velocity by regulating the off-rate of bonds between L-selectin and PSGL-1, thereby changing their lifetimes. To test this hypothesis, we measured transient tether lifetimes at 250 fps on low densities of monomeric sPSGL-1 ($<$10 sites/μm^2) that did not support rolling when measured at 30 or 250 fps. The tether lifetimes were used to derive off-rates (k_{off}), which were plotted against wall shear rate, wall shear stress, and tether force (Fig. 3). A faster camera speed of 500 fps generated identical data, indicating that the 250-fps speed was sufficient for accurate measurements. By contrast, a standard camera speed of 30 fps yielded lower apparent off-rates that reflected a failure to detect short tether lifetimes, although the plots obtained had the same shapes and same minimum positions (unpublished data). Like the rolling velocity curves, the k_{off} curves scaled with tether force but not with wall shear rate or with wall shear stress unless the spheres were the same size (Fig. 3). This is expected because kinetic off-rate at the molecular level should depend directly on force. That tether lifetime failed to scale with shear rate further excludes transport-dependent formation of new bonds as a mechanism to prolong tether lifetime at suboptimal flow rates. The off-rates most likely reported dissociations of single bonds because tether lifetimes were measured on very low densities of monomeric sPSGL-1 that did not support dimeric interactions (Marshall et al., 2003; Sarangapani et al., 2004). The off-rate curve closely matched previous data obtained with atomic force microscopy and with limited transient tether lifetime determinations (Sarangapani et al., 2004). The off-rate and rolling velocity curves shared the same shape, decreasing in tandem as force increased in the suboptimal range and increasing in tandem as force further increased above the optimal value. Indeed, the ratios of rolling velocity to off-rate were nearly constant, and were independent of

Figure 2. **Tether force governs rolling velocity below and above the flow optimum.** Mean velocities of L-selectin–bearing microspheres of 3- or 1-μm radii (A–C) or of unfixed or fixed neutrophils (D–F) rolling on sPSGL-1 (140 sites/μm^2) in the absence or presence of 6% Ficoll were plotted against wall shear rate, wall shear stress, and tether force. A logarithmic scale was used to plot the broad range of wall shear rates and wall shear stresses, whereas a linear scale was used to plot tether forces. The data represent the mean ± SD of five experiments.
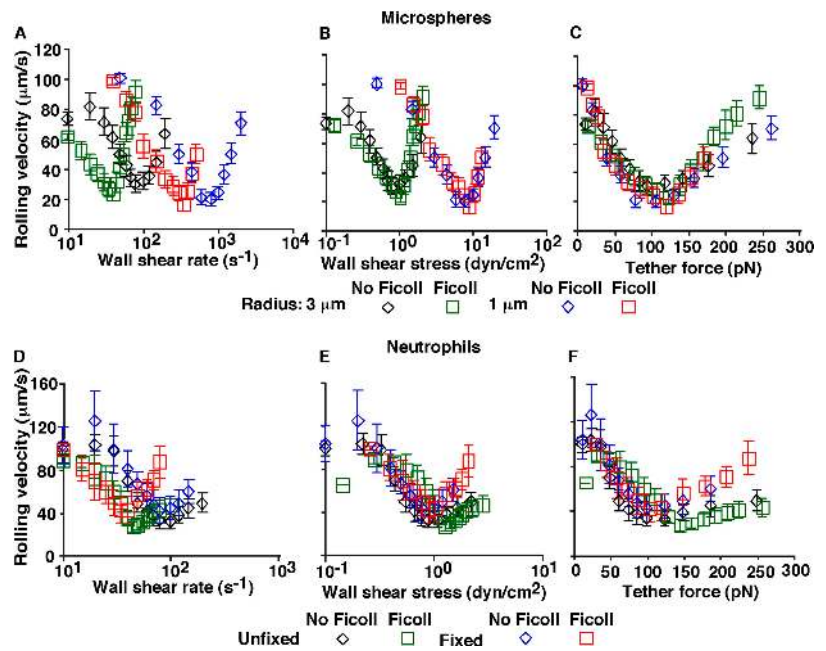

tether force across all conditions tested (unpublished data). This remarkable quantitative correlation suggests that transitions between catch bonds and slip bonds govern rolling velocity across the flow optimum. In particular, the optimal flow rate that provides the lowest rolling velocity is determined by the optimal tether force that provides the maximal lifetime for the L-selectin–PSGL-1 interaction, where it transits from a catch bond to a slip bond.

Transitions between catch bonds and slip bonds govern stop-and-go instantaneous velocities below and above the optimal force

Off-rate may regulate mean rolling velocity by controlling the time a sphere stops (pauses) between two consecutive movements, the frequency of the stops, and/or the relative

times the sphere spends in the stop and go phases. To test these hypotheses, we examined continuous rolling motions of individual microspheres and neutrophils recorded at high temporal resolution (250 fps). Frame-by-frame displacements were used to obtain time courses of instantaneous velocity. Fig. 4 illustrates the velocity profiles of representative microspheres of 3-μm radius rolling on sPSGL-1 for 1 s in media without Ficoll at tether forces below and above the optimum. The top left panel of Fig. 4 depicts the comparative velocity profiles of microspheres flowing over a human serum albumin (HSA)-coated surface at wall shear rates up to 50 s^{-1} (potential tether forces up to 60 pN), where velocity fluctuations of free-flowing particles could be accurately determined. The transient L-selectin–PSGL-1 interactions produced a cyclic stop-and-go pattern of rolling motions that

Figure 3. **Tether force governs off-rates of transient tethers below and above the flow optimum.** Off-rates (k_{off}) derived from lifetimes of transient tethers of L-selectin–bearing microspheres of 3- or 1-μm radii (A–C) or of unfixed or fixed neutrophils (D–F) to low density sPSGL-1 (<10 sites/μm^2) in the absence or presence of 6% Ficoll were plotted against wall shear rate, wall shear stress, and tether force. A logarithmic scale was used to plot the broad range of wall shear rates and wall shear stresses, whereas a linear scale was used to plot tether forces. The data represent the mean ± SD of five experiments.
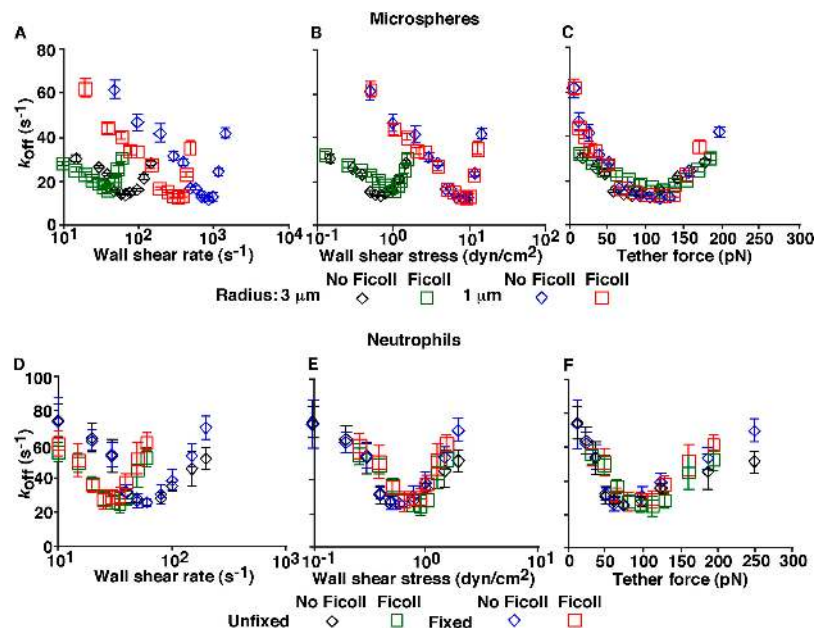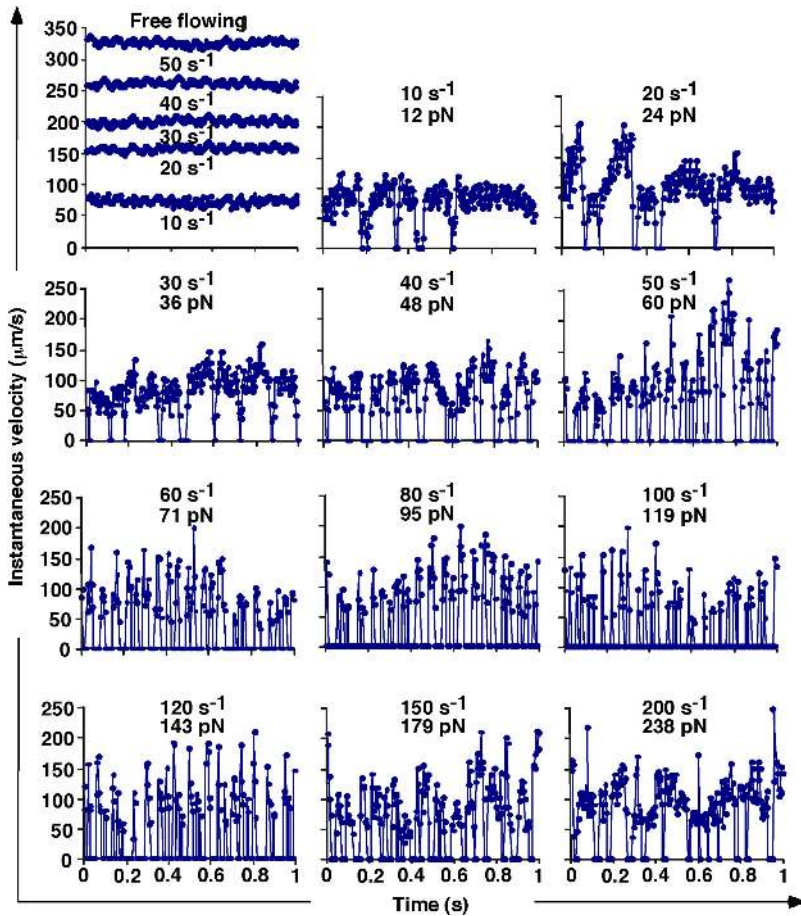
Figure 4. **Changing features of instantaneous rolling velocity below and above the flow optimum.** Shown are instantaneous velocities of representative L-selectin–bearing microspheres of 3-μm radii rolling on sPSGL-1 (140 sites/μm^2) in the absence of Ficoll at wall shear rates (s^{-1}) and corresponding tether forces (pN) below and above the optimum. The data were recorded at 250 fps. The top left panel shows the comparative instantaneous velocities of microspheres freely flowing over an HSA-coated surface at wall shear rates up to 50 s^{-1} (potential tether forces up to 60 pN), where velocity fluctuations could be accurately measured.

corresponded to the events modeled in Fig. 1 B. This gave rise to instantaneous velocities that fluctuated with periodic accelerations and decelerations over a much wider range than the narrow Brownian fluctuations in velocity of free-flowing microspheres. As flow increased, the free-flowing velocity profiles rose with similar fluctuation levels and no stops. By contrast, the rolling velocity time courses were punctuated by stops where the instantaneous velocity decreased to zero. Rolling at low flow rates was highly irregular, with frequent accelerations and decelerations of small magnitude but very few sporadic stops. These irregular motions resulted from weak and short-lived but specific interactions between L-selectin and PSGL-1, as they were readily distinguished from free-flowing motions. As force increased toward the optimal value, the velocity fluctuations intensified and became more regular. More decelerations converted into stops, which became longer, indicating progressively stronger and longer-lived interactions between L-selectin and PSGL-1. As flow increased beyond the optimal value, the trend was reversed. The velocity fluctuations diminished and became less regular. Fewer decelerations converted into stops, which became shorter, indicating progressively weaker and shorter-lived interactions between L-selectin and PSGL-1. Similar rolling profiles were obtained at 125 fps, demonstrating that the measurements had adequate temporal resolution. Profiles obtained at 83, 50, and 30 fps had progressively fewer fluctuations because more and more brief rolling steps failed to be detected (unpublished data). As a result, cells or micro-

spheres appeared to glide along the surface rather than to roll with a distinct stop-and-go pattern, indicating that these lower frame speeds lacked sufficient temporal resolution.

Transitions between catch bonds and slip bonds explain multiple parameters that quantify rolling behavior

To quantify the above observations (see Fig. 4), we segregated the 250-fps rolling time courses into stop and go phases as modeled in Fig. 1 B. A rolling step was defined as a cycle of acceleration and deceleration above a threshold that distinguished it from the narrow velocity fluctuations of free-flowing microspheres or neutrophils (see Materials and methods). Acceleration of a rolling microsphere or neutrophil indicated a decrease in the adhesive forces that resulted from dissociation of the rear-most bond(s). Deceleration indicated an increase in adhesive forces loaded on a bond(s) that formed between the chamber floor and the bottom of the microsphere or neutrophil as it was being translocated to the rear end. Note that the rolling step might or might not include a period of zero velocity that was defined as a stop. Although a rolling step without a stop remained in the go phase by definition, it represented a specific L-selectin–PSGL-1 interaction that lasted long enough to decelerate the rolling motion, but not to decrease the velocity to zero. Nearly a thousand stop and go events were collected from 10–15 microspheres or neutrophils that rolled continuously for 1 s at each flow rate. From these events we derived the following parameters: mean stop times, stop and go frequen-

Figure 5. **Quantification of rolling parameters below and above the flow optimum.** Stop frequencies (A), mean stop times (B), fractional stop times (C), go frequencies (D), fractions of steps with stops (E), and fractional go times (F) for 3-μm microspheres rolling on PSGL-1 or freely flowing over HSA in the absence of Ficoll were plotted against tether force (linear scale). The data were recorded at 250 fps.
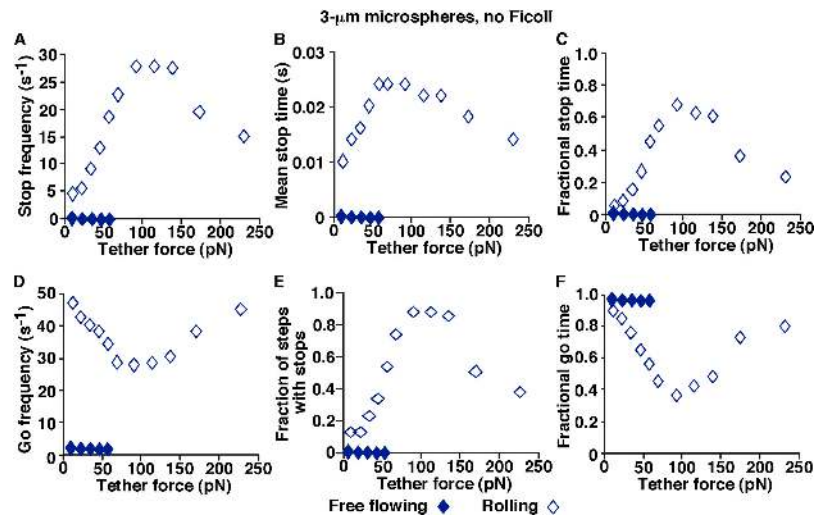
cies, fractional times spent in the stop or go phases, and fractions of steps with stops.

First, we analyzed 3-μm microspheres rolling on PSGL-1 or flowing freely over HSA in media without Ficoll. At flow rates where free-flowing velocities over HSA could be measured, the stop frequency was zero (Fig. 5 A), whereas the go frequency was unity because the microsphere remained in the go phase during the entire 1-s observation time (Fig. 5 D). Accordingly, the mean stop time (Fig. 5 B), the fractional stop time (Fig. 5 C), and the fraction of steps with stops (Fig. 5 E) were zero, whereas the fractional go time was unity (Fig. 5 F). This demonstrates that our method distinguished nonspecific flowing motions from specific rolling motions, which plotted as biphasic curves. The specific curves were readily explained by the off-rates of L-selectin–PSGL-1 interactions that exhibited transitions between catch and slip bonds. As flow increased across the optimal value, the mean stop time first increased and then decreased (Fig. 5 B), suggesting that transitions between catch and slip bonds govern lifetimes of transient tethers that arrested the spheres from the fluid stream, measured at very low PSGL-1 densities (Fig. 3), as well as lifetimes of rolling tethers that stopped the spheres from pivoting motions, measured at higher PSGL-1 densities. Mean rolling velocities (Fig. 2 C), transient tether off-rates (Fig. 3 C), and reciprocal mean stop times (reciprocal of Fig. 5 B) had similar biphasic curves and had the same tether force optimum. This suggests that both transient tethers and rolling tethers represented either single bonds or the same small number of bonds under our experimental conditions. The stop frequency for rolling microspheres first increased, reached a maximum, and then decreased (Fig. 5 A). Conversely, the go frequency first decreased, reached a minimum, and then increased (Fig. 5 D). The shapes of the stop and go frequency curves were complementary because the stop and go phases were mutually exclusive. In the catch bond regime, increasing force toward the optimal level produced stronger L-selectin–PSGL-1 bonds with less frequent premature dissociation. The longer-lived bonds allowed greater adhesive forces to develop, which more frequently decelerated the sphere motions into full stops and thus reduced the frequency of

entry into the go phase. In the slip bond regime, further increase in force beyond the optimal level produced weaker L-selectin–PSGL-1 bonds with more frequent premature dissociation. The shorter-lived bonds failed to allow sufficient adhesive forces to develop, which less frequently decelerated the sphere motions into full stops and thus increased the frequency of entry into the go phase. As a consequence of the changing mean stop time, stop frequency, and go frequency, the fractional time a microsphere spent in the stop phase first increased as the tether force rose to the optimum and then decreased as the tether force rose above the optimum (Fig. 5 C), whereas the fractional go time first decreased and then increased (Fig. 5 F).

The biphasic curve for fraction of rolling steps with stops revealed how transitions from catch bonds to slip bonds regulate rolling regularity (Fig. 5 E). At suboptimal flow rates, bonds were weak and short lived, which might cause a sphere to decelerate but not stop because their premature dissociation caused the sphere to accelerate to start the next rolling step. These bonds enabled a sphere to roll with lower instantaneous velocities of much wider fluctuations than a free-flowing particle, yet with few and sporadic stops, giving rise to the irregular velocity profile (Fig. 4). Increasing force toward the optimal level converted the weak and short-lived bonds to stronger and longer-lived bonds. This increased the fraction of steps with stops from nearly zero to >0.8 (Fig. 5 E), giving rise to the more regular velocity profile (Fig. 4). Increasing force beyond the optimal level reversed this trend, resulting in a decrease in the fraction of steps with stops and in the less regular velocity profile.

Scaling of rolling parameters with tether force excludes transport as a mechanism to govern rolling regularity

If transitions between catch and slip bonds primarily regulate rolling behavior, the biphasic curves of rolling parameters should scale with tether force, but not with wall shear rate or with wall shear stress unless the microspheres or cells are the same size. On the other hand, if increased bond formation by transport primarily regulates rolling behavior, the biphasic curves should scale with wall shear rate but not with wall shear stress or with tether force. If increased bond formation
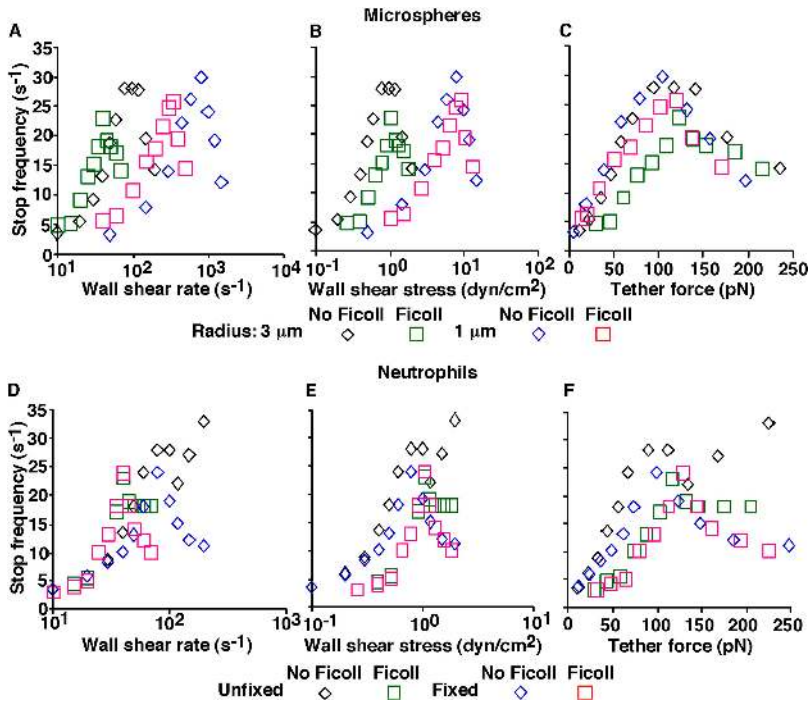
Figure 6. **Tether force governs rolling stop frequencies below and above the flow optimum.** Nearly a thousand stop events measured at 250 fps for each flow rate were collected from 10–15 L-selectin–bearing microspheres of 1- or 3-μm radii (A–C) or unfixed and fixed neutrophils (D–F), each continuously rolling for 1 s on sPSGL-1 (140 sites/ μm^2) in the absence or presence of 6% Ficoll. The stop frequencies were plotted against wall shear rate (logarithmic scale), wall shear stress (logarithmic scale), and tether force (linear scale).

by flattening of the cell contact area primarily regulates rolling behavior, changing deformability by fixing cells or using rigid microspheres should drastically alter rolling. To test these predictions, we measured the rolling parameters as a function of wall shear rate, wall shear stress, tether force, and cellular deformability by using media of different viscosities, rigid microspheres of different radii, and fixed and unfixed neutrophils. The plots of stop frequencies (Fig. 6) and mean stop times (Fig. 7) scaled with tether force, but not with wall

shear rate or with wall shear stress unless the spheres were the same size. The plots of go frequencies, fractional stop and go times, and fractions of steps with stops also scaled with tether force (unpublished data). The lack of scaling of these parameters with wall shear rate rules out transport as a mechanism to regulate rolling. Similar to Fig. 2 and Fig. 3, differences among plots of rigid microspheres, fixed neutrophils, and unfixed neutrophils were detectable but small, especially in the catch bond regime, ruling out increased bond formation
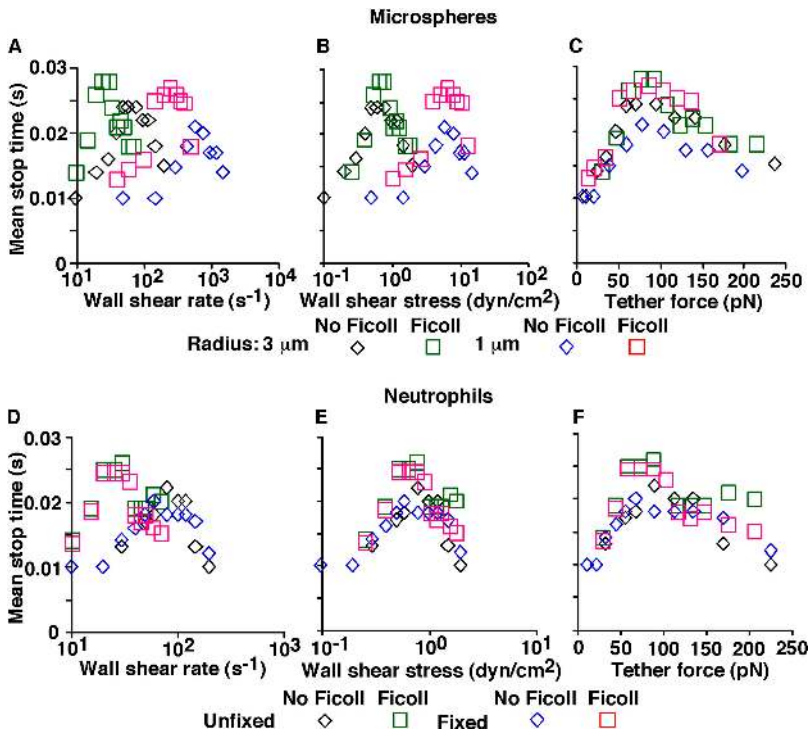

Figure 7. **Tether force governs rolling stop times below and above the flow optimum.** The mean stop times of the rolling microspheres and neutrophils described in Fig. 6 were plotted against wall shear rate (logarithmic scale), wall shear stress (logarithmic scale), and tether force (linear scale).

by flattening of the cell contact area as a major contributor to the shear threshold requirement. These combined data demonstrate that transitions between catch bonds and slip bonds govern both rolling velocity and rolling regularity across the tether force optimum. In particular, catch bonds enabled increasing force at suboptimal flow rates to convert weak, short-lived tethers into stronger, longer-lived tethers that increased the frequency and duration of stops.

Discussion

We have defined the first biological function for catch bonds, which lengthen their lifetimes in response to increasing force. The quantitative correlation of transient tether off-rates with mean rolling velocities and multiple measures of rolling regularity, and their parallel scaling with tether force, demonstrate that L-selectin uses catch bonds to decrease rolling velocity and increase rolling regularity as tether force increases from the threshold to the optimal level. These observations reveal catch bonds to be a key molecular mechanism for the flow enhancement of L-selectin–mediated cell adhesion (Finger et al., 1996; Alon et al., 1997).

As tether forces entered the catch bond regime, all curves that quantified rolling behavior were similar for rigid microspheres, fixed neutrophils, and unfixed neutrophils. The insensitivity to cell deformability indicates a direct effect of force on adhesive bond lifetime rather than an indirect effect of force on cellular features, which might increase the on-rates of adhesive bonds (Lawrence et al., 1997; Evans et al., 2001; Zhao et al., 2001). As tether forces entered the slip bond regime, mean rolling velocities rose more rapidly for microspheres and fixed neutrophils than for unfixed neutrophils. This represents the ability of fixation-sensitive cellular features to lower the effective force on adhesive bonds despite increasing wall shear stress (Yago et al., 2002). These cellular properties may include deformation that increases the adhesive contact area, facilitating new bonds that distribute the applied force, and extrusion of long membrane tethers that reduce the tether angle and thus the tether force (Firrell and Lipowsky, 1989; Shao et al., 1998; Lei et al., 1999; Schmidtke and Diamond, 2000; Rinker et al., 2001; Park et al., 2002; Smith et al., 2002). Cellular modulation of the force applied to slip bonds is particularly important at higher wall shear stresses than studied here, where more bonds are needed to maintain rolling (Chen and Springer, 1999; Smith et al., 2002; Yago et al., 2002). In contrast, molecular elasticity measurements reveal that applied force stretches L-selectin no more than 20 nm in the catch bond regime (unpublished data), which is insignificant relative to the micrometer dimensions for microvillous stretching and tether extrusion. At wall shear stresses below the optimal level, rolling is primarily regulated by molecular properties, specifically catch bonds, rather than by cellular properties.

In a recent report, off-rates derived from lifetimes of labile leukocyte tethers on L-selectin ligands measured at a 2-ms resolution were reported to be both high and insensitive to changes in flow until the threshold was reached, after which off-rates abruptly dropped independently of changes in viscosity (Dwir et al., 2003). The authors concluded that L-selectin tethers are stabilized by shear rate–dependent rotation of

leukocytes that increases bond number rather than by force-dependent prolongation of bond lifetime. We have been unable to confirm the results from this work. Our biphasic off-rate curves across the flow optimum tracked with tether force rather than wall shear rate, and we readily observed gradual rather than abrupt changes in the off-rates in both catch and slip bond regimes as flow increased. Furthermore, we measured the same force dependence for catch–slip transitional bonds between L-selectin and PSGL-1 using atomic force microscopy, a flow-independent method (Sarangapani et al., 2004). The discrepancies in our results and those of the previous work do not reflect differences in temporal resolution or in the choice of L-selectin ligands. We also observed catch–slip bond transitions when measuring tether lifetimes at a 2-ms resolution and on low densities of PNAd, a group of lymph node–derived ligands for L-selectin. The biphasic off-rate curves obtained on low density PNAd quantitatively correlated with the biphasic mean rolling velocity curves obtained on higher density PNAd, and both sets of curves scaled with shear stress rather than shear rate (unpublished data). The previous work did not examine whether shear rate or shear stress affected L-selectin–dependent rolling (Dwir et al., 2003). Significantly, we found that tether force, not shear rate, governed rolling velocity and rolling regularity below and above the flow optimum. We conclude that force-induced prolongation of L-selectin bond lifetime is essential for flow-enhanced cell adhesion. However, transport-induced increases in bond formation might also contribute to the shear threshold requirement. This may be especially important for flowing cells to tether, as increases in shear rate just above threshold levels might augment encounters between L-selectin and its ligands without unduly reducing the time required for molecular docking. Enhanced tethering by a transport mechanism might cooperate with catch bond stabilization of rolling to increase the number of adherent cells. Cells rolling irregularly at very low shears where bond lifetimes are still very brief might also rely on transport to form new bonds. Further analyses are required to address these possibilities.

Catch bonds might regulate other forms of flow-enhanced adhesion. Interactions of the bacterial adhesin FimH with mannosylated ligands promote adhesion of bacteria to epithelial surfaces under flow. Shear stress, but not shear rate, augments attachment of erythrocytes bearing FimH ligands to immobilized FimH-bearing bacteria (Thomas et al., 2002). The effect of shear stress is consistent with force-induced prolongation of FimH–ligand bonds, but it might also result from flattening of the erythrocyte contact area that favors new bonds. Therefore, well-controlled measurements of single bond dissociation under force are needed to determine whether FimH–ligand interactions indeed behave as catch bonds. Catch bonds might also explain why a minimum shear is required for the glycoprotein Ib complex to support platelet attachment to von Willebrand factor on disrupted vascular surfaces (Savage et al., 1996; Doggett et al., 2002). Under flow, catch bonds likely contribute most when the lifetimes of unstressed adhesive bonds are very short and when adhesion molecule densities are limiting. This would prevent inappropriate cell adhesion during stasis or undesired binding of a soluble ligand, whereas even a modest prolonga-

tion of bond lifetime might confer flow-enhanced adhesion. The shear threshold requirement for cell adhesion can be overcome by increasing adhesion molecule density or by molecular alterations that increase bond on-rates or decrease bond off-rates (Finger et al., 1996; Puri et al., 1998; Dwir et al., 2003). Leukocyte adhesion to P-selectin exhibits only a modest shear threshold requirement (Lawrence et al., 1997) because the lifetimes of P-selectin–PSGL-1 bonds are longer than those of L-selectin–PSGL-1 bonds (Alon et al., 1995, 1997; Mehta et al., 1998; Marshall et al., 2003; Sarangapani et al., 2004). However, very low forces do elicit catch bonds between P-selectin and PSGL-1, which might contribute to regulation of rolling at low flow rates (Marshall et al., 2003).

Determining how force-induced structural changes affect bond lifetimes remains a challenge for the future. A prototype may be how force applied to the COOH-terminal α-helix of the α_L-integrin I domain appears to stabilize its high affinity conformation and enable cell rolling under flow (Salas et al., 2002). Catch bonds may also affect cell properties in nonflow environments. Because virtually all adherent cells are subjected to mechanical stress, catch bonds could conceivably alter cell locomotion, spreading, and polarization. Catch bonds might also regulate interactions between molecular motors and cytoskeletal proteins (Veigel et al., 2003). Therefore, it is possible that catch bonds contribute to other biological functions that remain to be defined.

Materials and methods

Proteins and cells
The following proteins have been described: L-selectin–Ig containing the lectin domain, EGF domain, and both consensus repeats of human L-selectin fused to the Fc moiety of human IgG (Sarangapani et al., 2004), recombinant human sPSGL-1 (Yago et al., 2002), and anti–human PSGL-1 mAb PL1 (Yago et al., 2002). Anti–human IgG Fc pAb was from CHEMICON International. Anti–human L-selectin mAb DREG-56 was purified from hybridoma cells from the American Type Culture Collection. Human neutrophils were isolated as described previously (Ramachandran et al., 2001).

Coupling of L-selectin–Ig to microspheres and sPSGL-1 to flow chambers
Polystyrene microspheres (1- or 3-μm radius; Polysciences) were adsorbed with anti–human IgG Fc antibody in 500 μl HBSS, blocked with HBSS containing 1% HSA, and incubated with L-selectin–Ig. Microspheres were stored at 4°C in PBS containing 0.1% sodium azide for up to 5 d. The density of L-selectin, measured by flow cytometry with mAb DREG-56, remained constant during this period. Uniform L-selectin densities were maintained for all experiments. Neutrophils had 57,000 ± 7,000 ($n = 3$) L-selectin molecules per cell, as measured by binding of ^{125}I-labeled DREG-56 (Yago et al., 2002). The relative densities of L-selectin on neutrophils and microspheres were measured by flow cytometry. Assuming a smooth surface for each particle (which under-represents the surface area of neutrophils with their many microvilli), a neutrophil radius of 4.25 μm, and a uniform distribution of 57,000 L-selectin molecules on the surface of each neutrophil (which ignores the concentration of L-selectin on microvillous tips [Bruehl et al., 1996]), the L-selectin surface densities (sites/μm^2) were 251 for neutrophils, 707 for 3-μm microspheres, and 2,440 for 1-μm microspheres. Biotinylated sPSGL-1 was captured on streptavidin (Pierce Chemical Co.) adsorbed to flow chamber floors. Site densities of sPSGL-1 were determined by binding of ^{125}I-labeled PL1 (Yago et al., 2002).

Flow assays
Microspheres or neutrophils (10^6/ml in HBSS containing 1% HSA) were perfused at various flow rates over sPSGL-1 in a parallel-plate flow chamber (Ramachandran et al., 2001; Yago et al., 2002). To increase the viscosity in some experiments, 6% (wt/vol) Ficoll (400,000 M$_r$; Sigma-Aldrich) was added to the media. The viscosity of the media was measured as 1.0 cP (no Ficoll) or 2.6 cP (6% Ficoll of 400,000 M$_r$ or 9% Ficoll of 70,000

M$_r$) at RT in an Oswald dropping pipette viscometer (Fisher Scientific). In some experiments, microspheres or neutrophils were perfused in media containing 20 μg/ml DREG-56 or PL1 or 5 mM EDTA. All tethering and rolling events were specific because they were eliminated by inclusion of mAb or EDTA in the media.

Transient tether lifetimes were measured on low densities of sPSGL-1 that did not support rolling or skipping (Sarangapani et al., 2004). Images of transient tethers were captured with a Fastcam digital video camera (Super 10 K; Photron) at 250 or 500 fps. Images were replayed in slow motion, and durations of transient tethers were measured using frame-by-frame analysis. For each off-rate curve, five sets of lifetimes (~100 tethering events in each set) were measured at each wall shear stress. Off-rates were derived from each set as the negative slope of the linear fit to the ln (number of events with a lifetime ≥t) vs. t plot, which resulted in >0.9 correlation coefficients, R^2, for all fits. Off-rates were also estimated respectively from the reciprocals of the mean and SD of tether lifetimes (Marshall et al., 2003; Sarangapani et al., 2004), which gave consistent results.

Rolling step analyses
Mean rolling velocities were measured by tracking individual microspheres or neutrophils frame by frame (30 fps) with videomicroscopy with a 20× objective. Images were processed on a Silicon Graphics workstation using the Nanotrack analysis system in the Isee program (Isee Imaging Systems). The computer image algorithms mapped the digital image of a sphere to obtain subpixel resolution of its centroid (1 pixel = 0.625 μm at the magnification used). Rolling velocities were averaged over the period that the particles were tracked (Yago et al., 2002). For more detailed analysis of rolling behavior, images were continuously captured at 250 fps. The displacement of the sphere center along the flow direction in any two consecutive image frames was divided by the time elapsed (4 ms) between the two frames to calculate the instantaneous velocity, as exemplified in Fig. 4. To simulate camera speeds of 125, 83, 50, and 30 fps, only displacements in every other frame, every third frame, every fifth frame, and every eighth frame were selected and divided by the time elapsed (8, 12, 20, and 33 ms) between 3, 4, 6, and 9 frames to calculate instantaneous velocity. Several Excel (Microsoft) macros were written to further analyze these data using modifications of a previous method (Chen and Springer, 1999). The instantaneous velocity data were numerically differentiated to obtain the instantaneous acceleration. A step was defined as a cycle of acceleration and deceleration, which might or might not include a stop phase. A particle was defined to be in the stop phase if the instantaneous velocity was no greater than the mean noise level of the image analysis system, which was determined by tracking the instantaneous velocity of a set of stationary particles in a control experiment and was set at zero. Except for the lowest flow rates, all rolling steps resulted from specific L-selectin–PSGL-1 interactions because the particle velocities analyzed were far lower than those of particles freely flowing over HSA surfaces at the same shear (Fig. 4). At the low end of some curves, the mean velocity of a rolling particle was comparable to that of a free-flowing particle. To distinguish specific from nonspecific interactions under such conditions, a step was defined as a cycle of acceleration and deceleration whose magnitude exceeded a predetermined threshold. The threshold was chosen to separate acceleration and deceleration caused by dissociation and formation of bonds from those caused by Brownian fluctuations in velocity (Pierres et al., 2001). In the data in Figs. 5–7, a threshold of 2,500 μm/s^2 was chosen because the mean acceleration of a rolling particle was above 3,000 μm/s^2, whereas that of a free-flowing particle was below 800 μm/s^2. Threshold values above 1,000 μm/s^2 were sufficient to remove nearly all falsely identified pivot and stretch events from the velocity profiles of free-flowing particles. Threshold values ranging from 0 to 2,500 μm/s^2 yielded similar values for specific rolling parameters, indicating the ability to detect all but a negligible fraction of rolling steps mediated by the weakest specific interactions.

For each condition analyzed, the following statistics were calculated from nearly a thousand stop, go, and step segments segregated from 10–15 microspheres or cells, for each of which rolling at a given shear was continuously recorded for 1 s: stop and go frequencies, mean stop times, fractional stop and go times, and fractions of steps with stops.

Conversion from wall shear stress to tether force
To relate the force on the rear-most tether to wall shear stress, we measured lever arms for microspheres of 3-μm radii and for neutrophils by a flow reversal method (Yago et al., 2002). This method lacked sufficient resolution to accurately measure the lever arm for microspheres of 1-μm radii due to their small size. The conversion between wall shear stress and tether force for 1-μm microspheres was derived from that for 3-μm micro-

spheres by dimensional analysis. The motion of a sphere of radius r in a fluid of viscosity μ subject to a simple shear flow of shear rate $\dot{\gamma}$ near a planar surface can be described by the changes in time of the position x and rotational angle ψ (Fig. 1 A), which are governed by two equations that balance the respective forces and torques acted on the sphere (Tissot et al., 1992; Zhao et al., 2001):

$$
\begin{cases}
h_{11}\dfrac{d(x/r)}{d(\dot{\gamma}t)} + h_{12}\dfrac{d\psi}{d(\dot{\gamma}t)} = -1.7005 + \dfrac{F_t}{r^2\mu\dot{\gamma}}\dfrac{\cos\alpha}{6\pi} \\[2ex]
h_{21}\dfrac{d(x/r)}{d(\dot{\gamma}t)} + h_{22}\dfrac{d\psi}{d(\dot{\gamma}t)} = 0.4720 + \dfrac{F_t}{r^2\mu\dot{\gamma}}\dfrac{\cos(\alpha+\psi)}{8\pi}
\end{cases}
\tag{1}
$$

Eq. 1 has already been nondimensionalized by scaling x by r and t by $1/\dot{\gamma}$ such that all coefficients represent values for a sphere of unit radius, fluid of unit viscosity, and shear flow of unit shear rate. The drag coefficients h_{ij} ($i, j = 1, 2$) weakly depend on the gap distance between the sphere and the wall only; their values, which have been solved from fluid mechanics theory (Goldman et al., 1967), represent the forces (h_{1j}) and torques (h_{2j}) that the fluid exerts on the sphere due to its unit translation (h_{i1}) and rotation (h_{i2}) velocities. The first terms on the right-hand sides of Eq. 1 represent the force and torque due to shear. The last terms account for the fact that the sphere is tethered to the wall by a force F_t with an inclined angle α (Fig. 1 A), assuming that the rear-most tether provides all tensile force. $F_t = 0$ when the rear-most tether dissociates, which reduces Eq. 1 to a widely used theory (Goldman et al., 1967). In the presence of a tether, $F_t > 0$ is a function of x and ψ, and depends on tether properties. It seems reasonable that tether properties would be the same for microspheres of radii of 1 and 3 μm as they were mediated by the same molecular interactions, but would be different for microspheres and neutrophils because the latter have microvilli. It follows from Eq. 1 that rolling motions of microspheres of different radii in media of different viscosities subject to different shear rates are dynamically similar as long as they have the same dimensionless number $F_t/(r^2\mu\dot{\gamma})$. Physically, this number measures the relative importance of tether force and shear force. It increases as force develops and approaches maximum as the sphere approaches a complete stop when $d(x/r)/d(\dot{\gamma}t) = d\psi/d(\dot{\gamma}t) = 0$ (with corresponding parameters denoted by a subscript ∞),

$$
\frac{F_t}{r^2\dot{\gamma}} \rightarrow \frac{F_{t\infty}}{r^2\mu\dot{\gamma}} = \frac{32.05}{\cos\alpha_\infty} = \frac{11.86}{\cos(\alpha_\infty + \psi_\infty)}
\tag{2}
$$

which should be the same for microspheres of different radii but different for microspheres and neutrophils because their tethers have different properties. Eq. 2 also defines a relationship between α_∞ and ψ_∞. It follows from geometry (Fig. 1 A) that

$$
\frac{x_\infty}{r} = \sin\psi_\infty + \cot\alpha_\infty(1 - \cos\psi_\infty)
\tag{3}
$$

Using lever arm values measured from flow reversal experiments, $x_\infty/r = 0.344$ for 3-μm microspheres and 0.720 for 4.25-μm neutrophils, we can solve $\alpha_\infty = 75.9°$ and 62.3° for 3-μm microspheres and neutrophils, respectively, from Eq. 2 and Eq. 3. We then find from Eq. 2 $F_{t\infty}/(r^2\mu\dot{\gamma}) = 13.2$ and 6.89 for 3-μm microspheres and neutrophils, respectively. Because their tethers have the same properties, $F_{t\infty}/(r^2\mu\dot{\gamma})$ for the 1-μm microspheres should be the same as that for the 3-μm microspheres. Thus, the tether forces per unit wall shear stress are $F_{t\infty}/(\mu\dot{\gamma}) = 13.2$, 119, and 125 pN/(dyn/cm^2) for 1-μm microspheres, 3-μm microspheres, and 4.25-μm neutrophils, respectively. The lever arm values were insensitive to wall shear stress in the 0.5–2-dyn/cm^2 range tested where the conversion factors so determined would remain constants.

References

Alon, R., D.A. Hammer, and T.A. Springer. 1995. Lifetime of the P-selectin: carbohydrate bond and its response to tensile force in hydrodynamic flow. *Nature.* 374:539–542.

Alon, R., S.Q. Chen, K.D. Puri, E.B. Finger, and T.A. Springer. 1997. The kinetics of L-selectin tethers and the mechanics of selectin-mediated rolling. *J. Cell Biol.* 138:1169–1180.

Bell, G.I. 1978. Models for the specific adhesion of cells to cells. *Science.* 200: 618–627.

Bruehl, R.E., T.A. Springer, and D.F. Bainton. 1996. Quantitation of L-selectin distribution on human leukocyte microvilli by immunogold labeling and electron microscopy. *J. Histochem. Cytochem.* 44:835–844.

Chang, K.-C., and D.A. Hammer. 1999. The forward rate of binding of surface-tethered reactants: effect of relative motion between two surfaces. *Biophys. J.* 76:1280–1292.

Chen, S.Q., and T.A. Springer. 1999. An automatic braking system that stabilizes leukocyte rolling by an increase in selectin bond number with shear. *J. Cell Biol.* 144:185–200.

Dembo, M., D.C. Torney, K. Saxman, and D. Hammer. 1988. The reaction-limited kinetics of membrane-to-surface adhesion and detachment. *Proc. R. Soc. Lond. B. Biol. Sci.* 234:55–83.

Doggett, T.A., G. Girdhar, A. Lawshe, D.W. Schmidtke, I.J. Laurenzi, S.L. Diamond, and T.G. Diacovo. 2002. Selectin-like kinetics and biomechanics promote rapid platelet adhesion in flow: the GPIbα-vWF tether bond. *Biophys. J.* 83:194–205.

Dwir, O., A. Solomon, S. Mangan, G.S. Kansas, U.S. Schwarz, and R. Alon. 2003. Avidity enhancement of L-selectin bonds by flow: shear-promoted rotation of leukocytes turn labile bonds into functional tethers. *J. Cell Biol.* 163:649–659.

Evans, E., A. Leung, D. Hammer, and S. Simon. 2001. Chemically distinct transition states govern rapid dissociation of single L-selectin bonds under force. *Proc. Natl. Acad. Sci. USA.* 98:3784–3789.

Finger, E.B., K.D. Puri, R. Alon, M.B. Lawrence, U.H. Von Andrian, and T.A. Springer. 1996. Adhesion through L-selectin requires a threshold hydrodynamic shear. *Nature.* 379:266–269.

Firrell, J.C., and H.H. Lipowsky. 1989. Leukocyte margination and deformation in mesenteric venules of rat. *Am. J. Physiol.* 256:H1667–H1674.

Goldman, A.J., R.G. Cox, and H. Brenner. 1967. Slow viscous motion of a sphere parallel to a plane wall. II. Couette flow. *Chem. Eng. Sci.* 22:653–660.

Isberg, R.R., and P. Barnes. 2002. Dancing with the host: flow-dependent bacterial adhesion. *Cell.* 110:1–4.

Lawrence, M.B., G.S. Kansas, E.J. Kunkel, and K. Ley. 1997. Threshold levels of fluid shear promote leukocyte adhesion through selectins (CD62L,P,E). *J. Cell Biol.* 136:717–727.

Lei, X., M.B. Lawrence, and C. Dong. 1999. Influence of cell deformation on leukocyte rolling adhesion in shear flow. *J. Biomech. Eng.* 121:636–643.

Marshall, B.T., M. Long, J.W. Piper, T. Yago, R.P. McEver, and C. Zhu. 2003. Direct observation of catch bonds involving cell-adhesion molecules. *Nature.* 423:190–193.

McEver, R.P. 2001. Adhesive interactions of leukocytes, platelets, and the vessel wall during hemostasis and inflammation. *Thromb. Haemost.* 86:746–756.

McEver, R.P. 2002. Selectins: lectins that initiate cell adhesion under flow. *Curr. Opin. Cell Biol.* 14:581–586.

Mehta, P., R.D. Cummings, and R.P. McEver. 1998. Affinity and kinetic analysis of P-selectin binding to P-selectin glycoprotein ligand-1. *J. Biol. Chem.* 273:32506–32513.

Park, E.Y., M.J. Smith, E.S. Stropp, K.R. Snapp, J.A. DiVietro, W.F. Walker, D.W. Schmidtke, S.L. Diamond, and M.B. Lawrence. 2002. Comparison of PSGL-1 microbead and neutrophil rolling: microvillus elongation stabilizes P-selectin bond clusters. *Biophys. J.* 82:1835–1847.

Pierres, A., A.M. Benoliel, C. Zhu, and P. Bongrand. 2001. Diffusion of microspheres in shear flow near a wall: use to measure binding rates between attached molecules. *Biophys. J.* 81:25–42.

Puri, K.D., S. Chen, and T.A. Springer. 1998. Modifying the mechanical property and shear threshold of L-selectin adhesion independently of equilibrium properties. *Nature.* 392:930–933.

Ramachandran, V., T. Yago, T.K. Epperson, M.M.A. Kobzdej, M.U. Nollert, R.D. Cummings, C. Zhu, and R.P. McEver. 2001. Dimerization of a selectin and its ligand stabilizes cell rolling and enhances tether strength in shear flow. *Proc. Natl. Acad. Sci. USA.* 98:10166–10171.

Rinker, K.D., V. Prabhakar, and G.A. Truskey. 2001. Effect of contact time and force on monocyte adhesion to vascular endothelium. *Biophys. J.* 80:1722–1732.

Salas, A., M. Shimaoka, S. Chen, C.V. Carman, and T. Springer. 2002. Transition from rolling to firm adhesion is regulated by the conformation of the I domain of the integrin lymphocyte function-associated antigen-1. *J. Biol. Chem.* 277:50255–50262.

Sarangapani, K.K., T. Yago, A.G. Klopocki, M.B. Lawrence, C.B. Fieger, S.D. Rosen, R.P. McEver, and C. Zhu. 2004. Low force decelerates L-selectin dissociation from P-selectin glycoprotein ligand-1 and endoglycan. *J. Biol. Chem.* 279:2291–2298.

Savage, B., E. Saldívar, and Z.M. Ruggeri. 1996. Initiation of platelet adhesion by arrest onto fibrinogen or translocation on von Willebrand factor. *Cell.* 84:289–297.

Schmidtke, D.W., and S.L. Diamond. 2000. Direct observation of membrane tethers formed during neutrophil attachment to platelets or P-selectin under physiological flow. *J. Cell Biol.* 149:719–729.

Shao, J.Y., H.P. Ting-Beall, and R.M. Hochmuth. 1998. Static and dynamic lengths of neutrophil microvilli. *Proc. Natl. Acad. Sci. USA.* 95:6797–6802.

Smith, M.L., M.J. Smith, M.B. Lawrence, and K. Ley. 2002. Viscosity-independent velocity of neutrophils rolling on P-selectin in vitro or in vivo. *Microcirculation.* 9:523–536.

Thomas, W.E., E. Trintchina, M. Forero, V. Vogel, and E.V. Sokurenko. 2002. Bacterial adhesion to target cells enhanced by shear force. *Cell.* 109:913–923.

Tissot, O., A. Pierres, C. Foa, M. Delaage, and P. Bongrand. 1992. Motion of cells sedimenting on a solid surface in a laminar shear flow. *Biophys. J.* 61:204–215.

Veigel, C., J.E. Molloy, S. Schmitz, and J. Kendrick-Jones. 2003. Load-dependent kinetics of force production by smooth muscle myosin measured with optical tweezers. *Nat. Cell Biol.* 5:980–986.

Vestweber, D., and J.E. Blanks. 1999. Mechanisms that regulate the function of the selectins and their ligands. *Physiol. Rev.* 79:181–213.

Yago, T., A. Leppänen, H. Qiu, W.D. Marcus, M.U. Nollert, C. Zhu, R.D. Cummings, and R.P. McEver. 2002. Distinct molecular and cellular contributions to stabilizing selectin-mediated rolling under flow. *J. Cell Biol.* 158:787–799.

Zhao, Y., S. Chien, and S. Weinbaum. 2001. Dynamic contact forces on leukocyte microvilli and their penetration of the endothelial glycocalyx. *Biophys. J.* 80:1124–1140.